
This is an electronic reprint of the original article.
This reprint may differ from the original in pagination and typographic detail.

Author(s): Lipsanen, Harri & Sopanen, M. & Ahopelto, J.
Title: Luminescence from excited states in strain-induced In_xGa_{1-x}As quantum dots
Year: 1995
Version: Final published version

Please cite the original version:

Lipsanen, Harri & Sopanen, M. & Ahopelto, J.. 1995. Luminescence from excited states in strain-induced In_xGa_{1-x}As quantum dots. Physical Review B. Volume 51, Issue 19. P. 13868-13871. ISSN 1098-0121 (printed). DOI: 10.1103/physrevb.51.13868.

Rights: © 1995 American Physical Society (APS). <http://www.aps.org/>

All material supplied via Aaltodoc is protected by copyright and other intellectual property rights, and duplication or sale of all or part of any of the repository collections is not permitted, except that material may be duplicated by you for your research use or educational purposes in electronic or print form. You must obtain permission for any other use. Electronic or print copies may not be offered, whether for sale or otherwise to anyone who is not an authorised user.

Luminescence from excited states in strain-induced $\text{In}_x\text{Ga}_{1-x}\text{As}$ quantum dots

H. Lipsanen and M. Sopanen

Optoelectronics Laboratory, Helsinki University of Technology, Otakaari 1, FIN-02150 Espoo, Finland

J. Ahopelto

VTT Electronics, Otakaari 7, FIN-02150 Espoo, Finland

(Received 28 December 1994; revised manuscript received 27 February 1995)

We have fabricated quantum dots by locally straining $\text{In}_x\text{Ga}_{1-x}\text{As}$ quantum wells with self-organized growth of nanometer-scale InP stressors on the sample surface. The structure is completed in a single growth run using metalorganic vapor-phase epitaxy. Photoluminescence from the dots is redshifted by up to 105 meV from the quantum-well peak due to the lateral confinement of excitons. Clearly resolved luminescence peaks from three excited states separated by 16–20 meV are observed when the quantum well is placed at the depth of 1–10 nm from the surface of the sample. The observed redshift and peak separation are in agreement with simple calculations using a finite-element method and two-dimensional parabolic potential model. This structure is easily fabricated and offers a great potential for the optical study of relaxation and recombination phenomena.

Optical properties of zero-dimensional (0D) semiconductor structures, i.e., quantum dots (QD's), have attracted considerable experimental and theoretical interest in recent years.^{1–9} Various fabrication techniques of quantum dots have been proposed based on high-resolution patterning with or without subsequent regrowth,² on disordering induced by a laser³ or an ion beam,⁴ and on lateral strain modulation with stressors.^{5–8} However, these approaches require complex nanofabrication processes and, furthermore, process-induced inhomogeneities and adjacent regrown interfaces may severely affect the optical properties of the dots,⁹ as also reported for 2D quantum wells (QW's).¹⁰ The diminished luminescence efficiency of QD's has also been explained as an intrinsic effect due to reduced relaxation rate of carriers.¹¹

A direct method to produce defect-free quantum dots *in situ* is Stranski-Krastanow (SK) growth¹² which has been applied successfully on Ge/Si,¹³ $\text{In}_x\text{Ga}_{1-x}\text{As}/\text{GaAs}$,¹⁴ and InP/GaAs (Ref. 15) systems. In the SK growth coherent three-dimensional islands are formed on a thin two-dimensional wetting layer as the growth of the strained layer is interrupted just after exceeding its critical thickness, e.g., ~ 2 ML for InP/GaAs. Highly uniform buried $\text{In}_x\text{Ga}_{1-x}\text{As}$ dots with the diameter of 12–30 nm and the density of $\sim 10^{11} \text{ cm}^{-2}$ on GaAs have been reported,^{16–19} as well as photoluminescence (PL) of single InAs islands.²⁰ The shape transformation and intermixing during the growth of buried dots and the existence of the 2D wetting layer makes the modeling of these structures tedious and semiempirical. This can be avoided by combining the SK growth and the strain modulation of a QW as Sopanen, Lipsanen, and Ahopelto recently proposed.²¹ In the work the InP islands were grown *in situ* on the 30-nm-thick top barrier of an $\text{In}_x\text{Ga}_{1-x}\text{As}/\text{GaAs}$ quantum well. The method was shown to produce laterally confined quantum dots with high PL efficiency. With this approach the benefit of the SK growth in forming quantum-sized dots can be extended to materials where the direct island growth is not successful. Furthermore, the method is easy to implement and has an advantage that the high-quality 2D QW and the islands on the surface

are spatially separated. The possible intermixing and inhomogeneity of the islands lead only to slightly altered strain as discussed later. In this paper we report the PL data of structures with thinner GaAs top barriers than in Ref. 21, where excited-state luminescence becomes clearly resolvable. The results are compared to preliminary calculations with elastic finite element method (FEM) and a simple harmonic-oscillator model. We believe that this structure is promising for studying carrier relaxation and recombination processes, such as “phonon bottleneck” effect¹¹ in quantum dots due to the sharp PL lines from the excited states.

The samples were grown by metalorganic vapor-phase epitaxy (MOVPE) at atmospheric pressure. The layers were grown in a single growth run at 650 °C on semi-insulating (100)±0.5° GaAs substrates using trimethylgallium, trimethylindium, tertiarybutylarsine, and tertiarybutylphosphine without intentional doping.^{21,22} A 7-nm-thick $\text{In}_{0.25}\text{Ga}_{0.75}\text{As}$ quantum well was covered by a GaAs top layer with thicknesses ranging from 20 to 1 nm, followed by the growth of InP islands. The InP islands, which are acting as stressors, were about 100 nm wide and 20 nm high determined by atomic force microscopy and scanning electron microscopy. The island density was $2 \times 10^9 \text{ cm}^{-2}$. The size and density of the islands can be controlled in a very reproducible manner by changing the growth conditions.²³ Our previous study revealed a contribution of larger partially relaxed islands in photoluminescence²¹ but in this work such a signal was not observed. These larger islands are only formed when more than about 4 ML of InP are deposited.²³ The samples were cooled to 12 K in a closed-cycle helium cryostat and the PL spectra were measured with a 488-nm line from an argon-ion laser and a 77-K germanium *p-i-n* detector. The spot diameter was about 200 μm . Consequently, about 6×10^5 dots were excited.

The inset in Fig. 1 shows a schematic cross section of the sample. The strain field due to the SK grown InP stressors modulate the conduction and valence bands of the underlying material as presented in Refs. 5–8. The tensile strain below the stressors produces a laterally confined potential

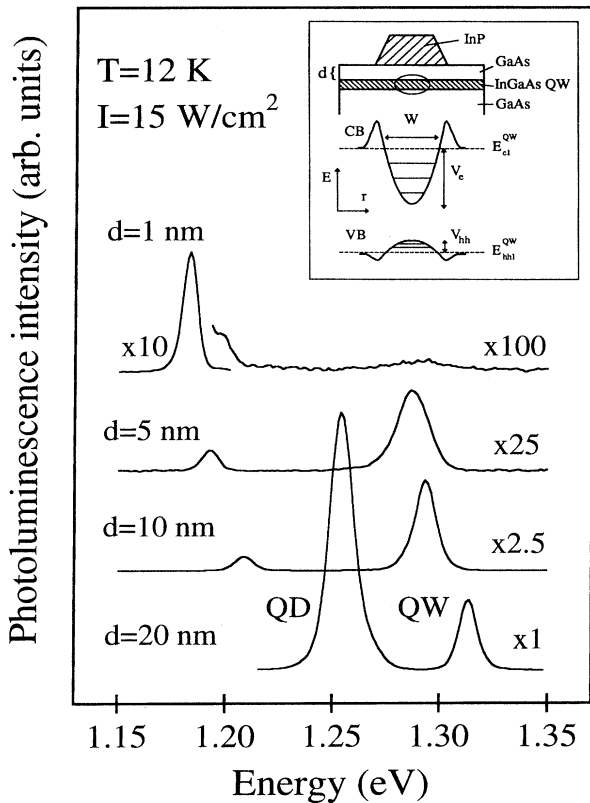


FIG. 1. PL of strain-induced quantum dots with various separations d from the stressing InP islands. Inset shows schematically the sample structure and the strain-induced band-edge modulation of the QW.

well into the $\text{In}_x\text{Ga}_{1-x}\text{As}$ QW, predominantly for electrons but also for holes. The local potential wells are approximately parabolic as shown in the inset. Close to the edges of the islands the strain is compressive, which causes an increased band gap. Figure 1 shows PL spectra of the sample with various top GaAs layer thicknesses d of 1–20 nm measured with the excitation intensity of 15 W/cm^2 . Two peaks are seen in each spectrum, a high-energy peak at around 1.3 eV from the ground-state heavy-hole transition of the unperturbed QW which serves as a reference and a peak at lower energy from the strain-induced QD's. As d is decreased both peaks shift to red and decrease in intensity. At the same time the separation of the QW and QD peak increases from 64 to 105 meV due to the increased effect of the strain field from the islands. The QW peak experiences an opposite shift than the reported blueshift for near-surface QW's.²⁴ This is believed to be due to the indium segregation during growth which lowers the top GaAs barrier band gap for low d 's.²⁵ In our previous work²¹ the origin of the QD peak was checked by measuring PL from a sample where the InP islands were selectively etched off. Moreover, similar structures without QW's show only a weak PL signal at $E \approx 1.40\text{--}1.45 \text{ eV}$. The full width at half-maximum (FWHM) of the QD peak decreases from 15 to 9 meV as d is reduced from 20 to 1 nm. At low values of d , the strain field in the QW tends to saturate, as deduced from the less rapidly increasing redshift.

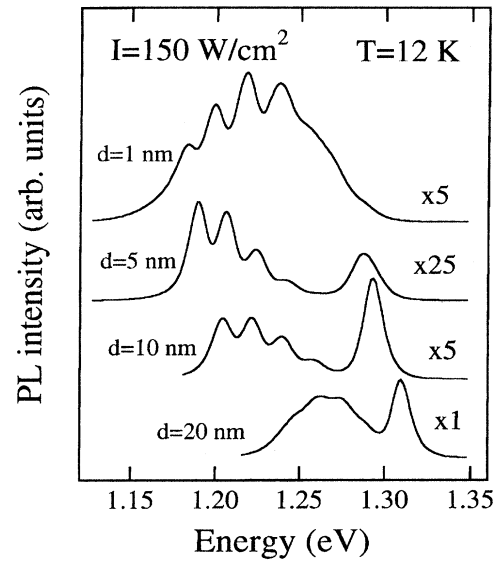


FIG. 2. PL from the samples at high excitation intensity of 150 W/cm^2 . The luminescence of the dots reveals well-resolved peaks from excited states. At the narrowest barrier of $d=1 \text{ nm}$ the ground-state dot luminescence is saturated.

The strain saturation reduces efficiently the effect of the size distribution of the stressor islands and, as a result, improves the size homogeneity of the strain-induced dots.

A small feature at 18 meV above the QD peak is barely visible in the PL spectrum of the $d=1 \text{ nm}$ sample in Fig. 1 measured at 15 W/cm^2 . By increasing the excitation intensity up to 150 W/cm^2 the spectra change dramatically as shown in Fig. 2. In addition to the lowest-energy QD peak up to four new peaks at increasing energy are revealed with nearly equal separation in each spectrum. The intensity ratio of the QD to QW peaks for $d \leq 10 \text{ nm}$ is increased as compared to Fig. 1 indicating an efficient carrier capture into the

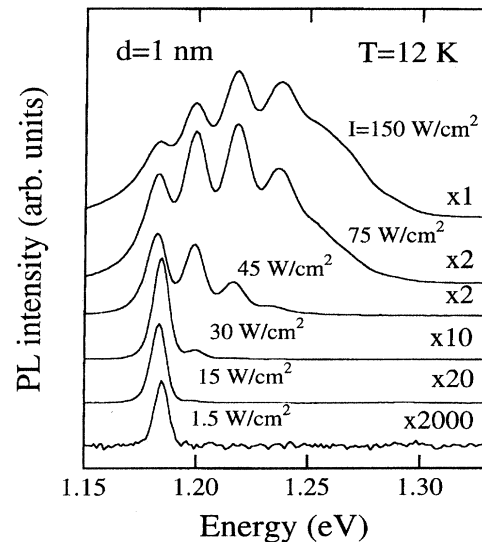


FIG. 3. State filling and consequent luminescence from excited states from the dots with $d=1 \text{ nm}$ as the excitation intensity is increased.

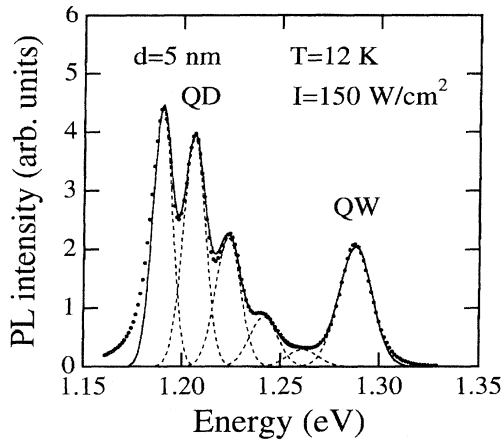


FIG. 4. PL spectrum of the $d=5$ nm sample at excitation intensity of 150 W/cm^2 shown by \bullet . A fitted curve (solid line) consists of five Gaussian fits to the QD peaks and a fit to the QW peak shown by dotted lines.

dots, in spite of the barrier at the edges of the dots which tends to hinder the carrier drift from the QW. The excited state luminescence of the $d=1$ nm sample with increasing excitation intensity is shown in Fig. 3. The first excited state can be resolved at 30 W/cm^2 , and at 45 W/cm^2 already the third excited state can be extracted. By further increasing the intensity the ground-state peak saturates and the excited peaks start to dominate. In Fig. 4 five Gaussian QD peaks and a QW peak are fitted to the PL spectrum of the $d=5$ nm sample at 150 W/cm^2 . A very good fit is obtained by using peak separations of 16.2, 17.4, 18.3, and 20 meV between successive peaks starting from the ground state. The FWHM of the QD peaks is from 7 to 11 meV which is of the same order as obtained from the QW with a thicker, $d=20$ nm barrier. Therefore, the confinement along the growth direction (z) of the 7-nm-wide $\text{In}_x\text{Ga}_{1-x}\text{As}$ layer determines the FWHM of the dot peaks, and no broadening due to the lateral dimensional variation of the strain-induced dots can be extracted. Narrow QW's produce broadened PL peaks due to the monolayer thickness fluctuation. Thus, the use of a very narrow QW to minimize the strain variation of the dots in the z direction would lead to broadened and overlapped PL peaks, as long as a high number of dots are excited.

The measured redshift, determined here as the energy difference between the QW and lowest QD luminescence peaks, and the QD peak splitting ΔE are plotted in Fig. 5 as a function of d . The variation in the separation of adjacent peaks decreases at larger d 's. The largest redshift of 105 meV and peak separation of 20 meV obtained in this work compare favorably to the highest redshift of 60 meV and a level separation of 2.1 meV reported recently for dots using processed carbon stressors.⁸ The strain obtained with SK-grown islands is much larger than can be obtained by deposition and etching of 2D stressor layers without generation of dislocations.¹³ The theoretical redshift was calculated using elastic finite element method for both conduction and heavy-hole valence bands,^{6,26} and include the confinement for the lowest dot states as discussed later. The results are compared to experimental values in Fig. 5. The calculations are well in agreement with the experimental redshift for low values of

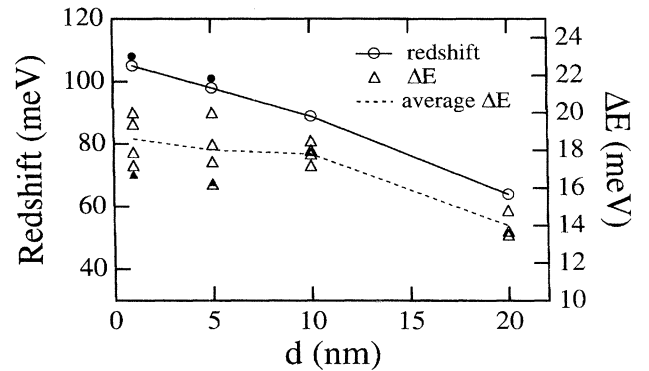


FIG. 5. Experimental redshift (\circ) and peak splitting ΔE (Δ) of adjacent peaks as a function of d . The lines are guide to an eye. The calculated values for the redshift and ΔE , shown by respective filled symbols, are close to the experimental values for $d=1$ and 5 nm.

d , but underestimate the redshift for larger d 's (not shown here) probably due to the deviation from the strain-induced parabolic band approximation.

The QD peak separation was calculated with a simple 2D infinite harmonic potential model using the values obtained from the FEM calculations for the potential well width W (at the lowest QW energy level) and the depth of the parabolic potential V_e and V_{hh} , as shown in Fig. 1. As a first approximation we neglect the Coulomb interaction between the electrons and holes as in Ref. 11. Therefore, the selection rule for radiative recombination is $\Delta_{n,l}=0$, where n is the radial quantum number (0,1,2, ...) and l is the angular momentum quantum number (0, $\pm 1, \pm 2, \dots$). The infinite rotational-symmetric parabolic potential $V_i = \frac{1}{2} m_i^* \omega_i^2 r^2$, where $i=e$ or h , ω_i is the characteristic frequency, m_i^* is the effective mass, and r is the radius of the potential, gives $\Delta E = \hbar \omega_e + \hbar \omega_h$ for the separation of adjacent radiative transitions. For instance, for the $d=5$ nm case the calculated W is 85 nm and V_e is 102 meV for electrons in $\text{In}_x\text{Ga}_{1-x}\text{As}$ ($m^*=0.056m_0$), which yields $\hbar \omega_e=12.4$ meV. For lateral "heavy" holes ($m^*=0.092m_0$), V_{hh} is 15 meV and $\hbar \omega_h=3.7$ meV is obtained. The experimental values of 98 meV and 16–20 meV for the redshift and peak separation, respectively, are close to the calculated redshift ($=V_e + V_{hh} - \hbar \omega_e - \hbar \omega_h$) of 103 meV and the separation of $\Delta E = 16.1$ meV. More detailed calculations will be published elsewhere.²⁷ These results suggest that the excited electrons and holes thermalize slowly to ground state and recombine also from excited states. The confinement energies for both types of carriers are larger than the longitudinal-acoustic-phonon energy (≤ 2 meV) (Ref. 3) but clearly smaller than the longitudinal-optical-phonon energy (~ 36 meV). This increases the carrier relaxation lifetime and causes the state filling which often leads to a broadened luminescence peak^{21,22} or to diminished luminescence.¹¹ However, the assumption in Ref. 11 that holes are readily thermalized to the ground state is not fulfilled here due to the larger hole level spacing, and both significant state filling and high PL efficiency are obtained. By further optimizing the structure even larger confinement can be achieved.

In conclusion, we have observed clear evidence of luminescence from excited states of strain-induced quantum dots.

The strain was applied to an $\text{In}_x\text{Ga}_{1-x}\text{As}$ quantum well by the self-organized growth of InP islands on top of the sample. The structures were fabricated *in situ* without any lithographic steps by MOVPE. A high PL efficiency was obtained from the strain-induced dots. The method produces quantum dots with good homogeneity as a consequence of the strain saturation for low barrier thicknesses. As the excitation intensity was increased close to 50 W/cm^2 the excited

state PL lines started to rise and the lower-lying lines saturated. The observed narrow (FWHM $\sim 8 \text{ meV}$) luminescence peaks from the dots with the separation of as high as 20 meV were redshifted by up to 105 meV from the QW peak, in consistence with our simple theoretical modeling. This structure offers an approach for the study of optical and electronic properties of quantum dots, especially the carrier relaxation and recombination processes.

- ¹U. Bockelmann, Phys. Rev. B **48**, 17 637 (1993).
- ²H. Temkin, G. J. Dolan, M. B. Panish, and S. N. G. Chu, Appl. Phys. Lett. **50**, 413 (1987); H. Temkin, L. R. Harriott, R. A. Hamm, J. Weiner, and M. B. Panish, *ibid.* **54**, 1463 (1989).
- ³K. Brunner, G. Abstreiter, M. Walther, G. Böhm, G. Tränkle, and G. Weimann, Phys. Rev. Lett. **69**, 3216 (1992).
- ⁴Y. Hirayama, Y. Suzuki, S. Tarucha, and H. Okamoto, Jpn. J. Appl. Phys. **24**, L516 (1985).
- ⁵K. Kash, J. M. Worlock, M. D. Sturge, P. Grabbe, J. P. Harbison, A. Scherer, and P. S. D. Lin, Appl. Phys. Lett. **53**, 782 (1988).
- ⁶I-H. Tan, R. Mirin, V. Jayaraman, S. Shi, E. Hu, and J. Bowers, Appl. Phys. Lett. **61**, 300 (1992).
- ⁷K. Kash, R. Bhat, D. D. Mahoney, P. S. D. Lin, A. Scherer, J. M. Worlock, B. P. Van der Gaag, M. Koza, and P. Grabbe, Appl. Phys. Lett. **55**, 681 (1989).
- ⁸K. Kash, D. D. Mahoney, B. P. Van der Gaag, A. S. Goddz, J. P. Harbison, and L. T. Florez, J. Vac. Sci. Technol. B **10**, 2030 (1993).
- ⁹K. Kash, J. Lumin. **46**, 69 (1990).
- ¹⁰K. Brunner, G. Abstreiter, G. Böhm, G. Tränkle, and G. Weimann, Appl. Phys. Lett. **64**, 3320 (1994).
- ¹¹H. Benisty, C. M. Sotomayor-Torrès, and C. Weisbuch, Phys. Rev. B **44**, 10 945 (1991).
- ¹²I. N. Stranski and L. Von Krastanow, Akad. Wiss. Lit. Mainz Math. Naturwiss. Kl. Iib **146**, 797 (1939).
- ¹³D. J. Eaglesham and M. Cerullo, Phys. Rev. Lett. **64**, 1943 (1990).
- ¹⁴S. Guha, A. Madhukar, and K. C. Rajkumar, Appl. Phys. Lett. **57**, 2110 (1990).
- ¹⁵J. Ahopelto, A. A. Yamaguchi, K. Nishi, A. Usui, and H. Sakaki, Jpn. J. Appl. Phys. **32**, L32 (1993).
- ¹⁶D. Leonard, M. Krishnamurthy, C. M. Reaves, S. P. DenBaars, and P. M. Petroff, Appl. Phys. Lett. **63**, 3203 (1993).
- ¹⁷J. M. Moison, F. Houzay, F. Barthe, L. Leprince, E. André, and O. Vatel, Appl. Phys. Lett. **64**, 196 (1994).
- ¹⁸J. Oshinowo, M. Nishioka, S. Ishida, and Y. Arakawa, Appl. Phys. Lett. **65**, 1421 (1994).
- ¹⁹D. Leonard, M. Krishnamurthy, S. Fafard, J. L. Merz, and P. M. Petroff, J. Vac. Sci. Technol. B **12**, 1063 (1994).
- ²⁰J.-Y. Marzin, J.-M. Gérard, A. Izraël, D. Barrier, and G. Bastard, Phys. Rev. Lett. **73**, 716 (1994).
- ²¹M. Söpanen, H. Lipsanen, and J. Ahopelto, Appl. Phys. Lett. (to be published).
- ²²M. Söpanen, H. Lipsanen, and J. Ahopelto (unpublished).
- ²³M. Söpanen (unpublished).
- ²⁴J. Dreybrodt, A. Forchel, and J. P. Reithmeier, Phys. Rev. B **48**, 14 741 (1993).
- ²⁵J.-M. Gerard and J.-Y. Marzin, Phys. Rev. B **45**, 6313 (1992).
- ²⁶K. Kash, B. P. Van der Gaag, D. D. Mahoney, A. S. Goddz, L. T. Florez, J. P. Harbison, and M. D. Sturge, Phys. Rev. Lett. **67**, 1326 (1991).
- ²⁷J. Tulkki and A. Heinämäki (unpublished).